Xiang Yu[1]
Hong-bo Shao[2, 3, 4]
Xiang-hua Liu[5]
Dong-zhi Zhao[6]

[1]Shandong Provincial Key Laboratory of Eco-environmental Sciences for the Yellow River Delta, Binzhou University, Binzhou P. R. China.

[2]Institute of Soil and Water Conservation, Chinese Academy of Sciences (CAS), Yangling, P. R. China.

[3]Yantai Institute of Coastal Zone Research, Chinese Academy of Sciences (CAS), Yantai, P. R. China.

[4]Institute for Life Sciences, Qingdao University of Science and Technology (QUST), Qingdao, P. R. China.

[5]The No.11 Middle School of Yantai, Yantai, P. R. China.

[6]National Marine Environment Monitoring Center, Dalian, P. R. China.

Research Article

Applying Neural Network Classification to Obtain Mangrove Landscape Characteristics for Monitoring the Travel Environment Quality on the Beihai Coast of Guangxi, P. R. China

The spectral characteristics of mangroves on the Beihai Coast of Guangxi, P. R. China are acquired on the basis of spectral data from field measurements. Following this, the 3-layer reverse-conversing neural networks (NN) classification technology is used to analyze the Landsat TM5 image obtained on January 8, 2003. It is detailed enough to facilitate the introduction of the algorithm principle and trains project of the neural network. Neural network algorithms have characteristics including large-scale data handling and distributing information storage. This research firstly analyzes the necessity and complexity of this translation system, and then introduces the strong points of the neural network. Processing mangrove landscape characteristics by using neural network is an important innovation, with great theoretical and practical significance. This kind of neural network can greatly improve the classification accuracy. The spatial resolution of Landsat TM5 is high enough to facilitate the research, and the false color composite from 3-, 4-, and 5-bands has a clear boundary and provides a significant quantity of information and effective images. On the basis of a field survey, the exported layers are defined as mangrove, vegetation, bare land, wetlands and shrimp pool. TM satellite images are applied to false color composites by using 3-, 4-, and 5-bands, and then a supervised classification model is used to classify the image. The processing method of hyper-spectrum remote sensing allows the spectral characteristics of the mangrove to be determined, and integrates the result with the NN classification for the false color composite by using 3-, 4-, and 5-bands. The network model consists of three layers, i.e., the input layer, the hidden layer, and the output layer. The input layer number of classification is defined as 3, and the hidden layers are defined as 5 according to the function operation. The control threshold is 0.9. The training ratio is 0.2. The maximum permit error is 0.08. The classification precision reaches 86.86%. This is higher than the precision of maximal parallel classification (50.79%) and the spectrum angle classification (75.39%). The results include the uniformity ratio (1.7789), the assembly ratio (0.6854), the dominance ratio (−1.5850), and the fragmentation ratio (0.0325).

Keywords: Environmental quality monitoring; Hyper-spectrum nerve network; Image classification; Landscape characteristics

Received: September 9, 2009; *revised:* November 16, 2009; *accepted:* January 3, 2010

DOI: 10.1002/clen.200900195

1 Introduction

The mangrove eco-system is one of the important systems on the seashore zone. It is known to have great effects on environmental protection, the ecosystem balance and the biological diversity of the seashore zone [1]. To date, many experts have used remote sensing technology to study mangrove systems. The most applied data system is a LandSat TM satellite because of its high performance-price ratio, e.g., the LandSat TM satellite data (spatial resolution = 30 m), SPOT XS satellite data (spatial resolution = 20 m) and PAN + XS satellite data (spatial resolution = 10 m) have been used to explore the distribution patterns of the mangroves on the Waite-Mata Harbor in western New Zealand: firstly, to sample the multi-soil types, and then to categorize the image by using supervised classification. The results indicate that the best precision is gained by the Land Sat TM satellite data (spatial resolution = 30 m) [2, 3]. Another use is to take the ratio ((5 − 7)/(5+7)) of the near-infrared bands 5 and 7 of the Land Sat TM satellite data as the index for classification [4]. A 3 * 3 edge

Correspondence: Prof. Dr. H.-B. Shao, Institute for Life Sciences, Qingdao University of Science & Technology (QUST), Qingdao 266042, P. R. China.
E-mail: shaohongbochu@126.com

swell filter can be adopted to distinguish the edges of the different mangrove forests for the targeted classification [5, 6], to differentiate the forest vegetation by the BPNN classification based on the data of Land Sat 7ETM+ and other maps of forest resources distribution [7, 8], and consequently, to develop new remote sensing classification technology based on the fuzzy quantitative analysis and multi-layer forward feedback NN (MLP) [9]. The data area is a multicolor-infrared remote navigation sensing image with the research area being the park-section; the precision reaches 78%. The result of application of a supervised classification and NN classification on the salt water area indicates that the NN classification is suitable for remote sensing classification and its precision is high enough for resource surveying [10].

Back propagation NN classification (BPNN) based on Landsat TM5 data is used to obtain the land cover classification and the result indicates the classification precision of BPNN reaches 87.90%, which is higher than the classification precision max-likelihood classifier, with a value of 83.22% [11]. A BP neural network is used to reconstruct a high spatial resolution remote sensed image from low spatial resolution images sequences. The procedure is introduced and the algorithm is verified by means of the experiment datum. The result shows the improved K-means algorithm is better than ACA algorithm and the simple K-means algorithm [12] A fuzzy neural network image classification is proposed. The back-propagation algorithm is employed to obtain the trained parameters of the fuzzy models. The Landsat-TM image data are used to inspect the effect of the proposed classifier. In comparison to the BP neural network classifier, the proposed model requires less learning time and results in more accuracy [13]. Rapid and accurate LAI retrieval from a large area is an important research topic in the field of remote sensing. In this paper, a model is presented to estimate the LAI of reed canopy from Landsat-5 TM image data. The model first classifies the background of reed canopy into soil and water and then calculates and outputs a lookup table (LUT) by use of an FCR model. Following this, LAI mapping is conducted based on the BP neural network model, which is trained using the data from the actual measurement and LUT. The result shows that the BP neural network model is better than others [14]. Based on the Land Sat TM satellite data (spatial resolution = 30 m), the NN classification is used to obtain the characteristics of the mangrove topography of Shankou, Guangxi, China, which is one of the best areas of scenery in the world.

2 Materials and Methods

2.1 Spectrum Materials

The Shankou mangrove resource protection section of Guangxi, lies in Beihai City, Guangxi, P. R. China. Its location lies at east longitude 109°37′ – 109°47′and north latitude 21°28′ – 21°37′. The physical features of this section mostly consist of an ancient pluvial mesa. A gulf coastal plain lies alongside the edge of the pluvial mesa, the modern shoreline and a small inlet. A few cliffs that are eroded by sea water lie on a segment of the Yingluo Harbor shoreline. The stratum class of this section is loose sedimentary material, olive basalt, and radix lava. The yearly range of air temperature over the Shankou mangrove resource protection section is 13.8°C. The extreme high is 38.2°C, and the extreme low is 1.5°C.

The spectrum curves of 5 varieties of mangrove as well as other objects were recorded by a VF921B SPECTRO SORT on a sunny day. The atmosphere temperature was 20°C and the intensity of illumination was 860 LX. The spectrum range of the VF921B SPECTRO SORT was 400 – 1000 nm, and the spectrum differentiate ratio was 5.4 nm, while the instantaneous field angle was ca. 10° and the auto range was ≥70 db. In order to minimize the error, the lens must be set at an angle of 45° to the sunlight. The effects of the water and shadowy objects are thus avoided by the hyper-spectrum analysis technology including logarithmic transformation and differential transforming.

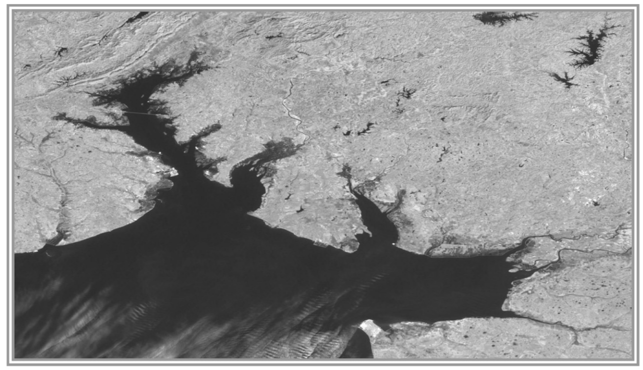

Figure 1. Land Sat TM5 satellite image of Beihai City of Guangxi, China. The image is an entire wide satellite depiction, and may be cut to fit the research requirements. This can cut the quantity of operation steps and improve the operation rate.

2.2 Image Materials and Correction

The image materials of this research include Land Sat TM5, which was obtained on January 8, 2003, by the China Remote Sensing Satellite Ground Station, were 1:50000 topographic maps and layout maps of the mangrove reserve, and these were obtained by the country resource office of Guangxi, China. In addition, the digital vector data was obtained by the Arc-view software of the geographical information system. The Land Sat TM5 image of the area on the Beihai Coast of Guangxi, P. R. China, is shown in Fig. 1.

At first, the digital vector data is obtained by the Arc-view software of the geographical information system based on the 1:50000 topographic maps of Beihai City of Guangxi, China. Following this, 20 reference points are selected, which are obvious enough on the vector maps corresponding to the Land Sat TM5 satellite image of China's Beihai City, in an attempt to correct the Land Sat TM5 satellite image on the remote sensing image processing software ENVI base level. The admitted cell error is 0.08, which is favorable. Following this, for the purpose of calculation rapidity, an area that overshadows the Shankou mangrove resource protection section is interpreted to fit the research work.

2.3 Spectrum Character Achievement Methods

On the basis of the original data, the expression below is used to obtain the spectrum character of 5 kinds of mangrove, Eq. (1):

$$S_m = \frac{S_t}{S_p} R_p \qquad (1)$$

where S_m is the spectrum of the mangrove or other objects, S_t is the original data, which is gained by VF921B SPECTRO SORT, S_p is the spectrum data of the reference board and R_p is the reflectivity of the reference board. The spectral differences in the visible region of the objects are enhanced by logarithmic transformation of the spectrum curves. The spectral background noise of the spectrum curves is avoided by the hyper-spectrum analysis technology. The spectrum values in the visible region are much lower than the spectrum value obtained by logarithmic transformation, and the refulgence of square resistance factors for the spectrum value also tends to be weakened. The expressions to summarize this situation are as follows, Eqs. (2) and (3):

$$r = A\,S_i \tag{2}$$

$$\log(r_i) = \log(A) + \log(S_i + B/A) \tag{3}$$

where S_i is the spectrum value, A is the square resistance factors and B represents the plus resistance factors. The three methods for differentiating the spectrum character of 6 kinds of vegetation are described below [11].

2.3.1 Spatial Distance

Each spectrum curve is configured by the reflection of given bands to make up a space vector, and to calculate their spatial distance, according to Eq. (4):

$$Q(X, P_i) \geq Q(X, P_1);\ R = \sum_{j=1}^{n} \pi_i (X - X_j)^2;\ Q = \sqrt{R};\ \pi_i = 1 \tag{4}$$

2.3.2 Correlativity

In addition, the correlativity can be used to differentiate the spectrum character of the vegetation, and can be given by Eq. (5):

$$\rho_{x,y} = \frac{Cov(X,Y)}{\sigma_x \sigma_y};\ Cov(X,Y) = \frac{1}{n}\sum_{j=1}^{n}(x_j - \mu_x)(y_j - \mu_y);$$

$$-1 \geq \rho_{x,y} \geq 1 \tag{5}$$

2.3.3 Spectrum Angle

The spectrum angle of each curve, as configured by the band reflection can be explained using Eq. (6):

$$\partial = \cos^{-1}\left[\frac{\sum_{i=1}^{n_b} t_i r_i}{\left(\sum_{i=1}^{n_b} t_i^2\right)^{\frac{1}{2}} \left(\sum_{i=1}^{n_b} r_i^2\right)^{\frac{1}{2}}}\right] \tag{6}$$

where n_b is the number of bands, t_i is the target spectrum, and r_i is the reference spectrum.

2.4 NN Classification Technology

2.4.1 The Structure of the NN Classification

Each input joint is supposed to delegate a component of the spectrum value, and each output joint delegates one type. For that reason, the number of hidden layers is shown in the expression given in Eq. (7):

$$N = \frac{A \times B + \frac{1}{2} A \times (B^2 + B) - 1}{A + B} \tag{7}$$

where A is the number of classification and B is the number of eigenvectors. If the motivation function of the network joint is Sigmoid type, then the relationship of the input and output can be described as follows. The input joint of the input layer is each component of the spectrum value, the output joint O_j, $O = X$, the input knot of the hidden layer is shown by I_j, and W_{ji} is the weight, as summarized by Eq. (8):

$$I_j = \sum W_{ji} O_i \tag{8}$$

The output of the hidden layer is given by O_j, as summarized in Eq. (9):

$$O_j = \frac{1}{i + \exp(-I_j)} \tag{9}$$

The input knot of the hidden layer is represented by I_k, W_{kj} is the weight. $I_k = \sum W_{kj} O_j$; and the output of the hidden layer is given by O_k, Eq. (10):

$$O_k = \frac{1}{i + \exp(-I_k)} \tag{10}$$

2.4.2 The Training Study Arithmetic Pattern

The study error function is defined by J_c according to Eq. (11):

$$J_c = \frac{1}{2}(D - Y)^T (D - Y) \tag{11}$$

where D is the anticipation value and Y is the exact output of the network. It follows that a value for W_{ji} is deduced. The term η is the study ratio [8] and is given by Eq. (12):

$$W_{ji}(t+1) = W_{ji}(t)\eta \frac{\partial j_C}{\partial w_{ji}} = W_{ji}(t)\eta \sum_{k}$$

$$\left[-(D_k - Y_k) \rightarrow \leftarrow \frac{\exp(-I_k)}{[1 + \exp(-I_k)]^2} W_{kj}\right] \frac{\exp(-I_j)}{[1 + \exp(-I_j)]^2} O_i \tag{12}$$

2.4.3 Arithmetic Pattern Achievement

NN is made up of 3 different layers, composed of the import layer, the hidden layer, and the export layer. The number of hidden layers affects the scale of NN. If the number is excessive, then NN is more complex; and the swatch character is easily obtained. However, the operation quantity is highly improved, but the demand time is excessively long. The import layer is the pivotal factor that affects the precision. The import layer gene must be exact and meet a definite quantity. On this point, the import layer must also meet the requirement to have a spectrum character difference. Since the space differentiation ratio of the artificial color image synthesis made up of the 3-, 4- and 5-bands of the Land Sat TM5 is favorable, the layer of the image is sufficient, and the field of the objects is also very clear. By contrasting the reflectivity of the bands of the Land Sat TM5 image, the best combination is selected. It is found that the correlation of 3-, 4-, and 5-bands is the smallest, and the quantity of information is sufficient. Therefore, the 3-, 4-, and 5-bands of the Land Sat TM5 satellite image are chosen, and the export layer is intercalated to band 5, including the mangrove, land vegetation, exposed land, water and shrimp pond. The image characteristic of the mangrove is bright green, and its distribution presents a mostly continuous zone, which is along the shoreline. It clearly differs from the water, but hardly differs from the grass around it. The

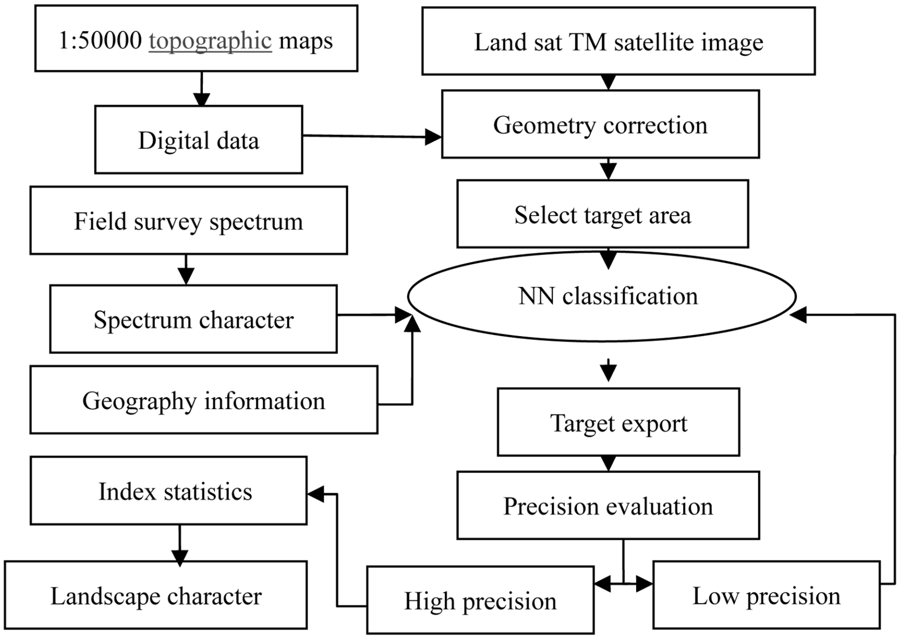

Figure 2. NN image classification operation flow diagram.

image characteristic of the land vegetation is bottle green, and its distribution also presents a continuous zone. However, it always has a dense concentration of brown stains or spots, which are exposed land or manmade buildings. The water is dark, and the shrimp pond is interposed into the water in a gridiron pattern. According to the precision contrast, based on actual flow operation and survey materials, the training threshold is 0.9, the training ratio is 0.2, the training time is 1000, and the maximum cell admit error is 0.1.

In order to make the standard swatch, bands 3, 4 and 5 are synthesized and the objects are sampled. Then the image is classified on the remote sensing image processing software ENVI base level. The overall operation flow is shown in Fig. 2.

2.5 Index Achievement

The index achievement parameters are defined in the following subsections.

2.5.1 Landscape Diversity Index, (*H*)

The landscape diversity index, H, is given by Eq. (13):

$$H = -\sum_{k=1}^{m} (P_k) \log_2 (P_k)^* \tag{13}$$

where P_k is the proportion ratio of k types of the whole area, and m is the number of landscape types.

2.5.2 Predominance Index, (*D*)

The predominance index, D, is given by Eq. (14):

$$D = H_{max} + \sum_{k=1}^{m} (P_k) \log_2 (P_k); H_{max} = \log_2 (P_k) \tag{14}$$

where P_k is the proportion ratio of k types of the whole area, and m is the number of landscape types. H_{max} is the maximum diversity index, which has the same proportion of each type of landscape.

2.5.3 Uniformity Index, (*E*)

The uniformity index, E, is given by the terms in Eq. (15):

$$E = (H/H_{max}) \cdot 100; H = -\log \left[\sum_{k=1}^{m} (P_k)^2 \right]; H_{max} = \log(m) \tag{15}$$

2.5.4 Landscape Fragmentation Index [15]

The landscape diversity fragmentation index is given by the terms in Eq. (16) [15]:

$$FN_1 = (N_p - 1)/N_c; FN_2 = \mathrm{MPS}\,(N_f - 1)/N_c \tag{16}$$

where N_c is the minimum grid of the image, N_p is the average spot acreage, and N_f is the type totality of a certain view.

2.5.5 Assembly Index

The assembly index is described by the terms in Eq. (17):

$$RC = 1 - C/C_{max}; C = -\sum_{i=1}^{m} \sum_{j=1}^{m} P(i,j) \log[P(i,j)];$$

$$C_{max} = m \log(m); P(i,j) = EE(i,j)/Nb \tag{17}$$

3 Results and Discussion

3.1 Mangrove Spectrum Characteristics

The spectra of the five types of mangrove are shown in Fig. 3. In mangrove spectrum characteristics research, VF921B SPECTRO SORT is used to obtain the original data, then the data is analyzed by hyper-spectrum analysis technology to obtain precise characteristics. Firstly, the logarithm transform of the curve is obtained, and in this way, the difference of spectrum value at the visible bands is

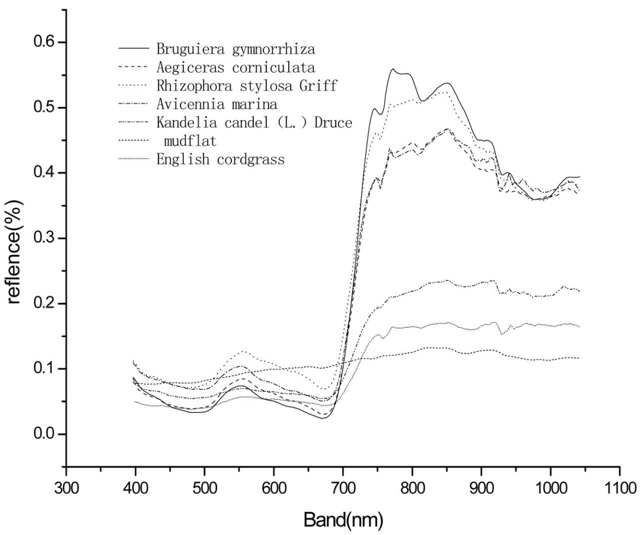

Figure 3. The spectra curves of 7 kinds of objects. The spectra curves are in the following order: *Bruguiera gymnorrhiza* (L.), *Aegiceras corniculata*, *Rhizophora stylosa* Griff, *Avicennia marina*, *Kandelia candel* (L.) *Druce*, Mudflat and English cordgrass.

also seen, and therefore, the calculus transform of the curve of the logarithm transform can be generated. This method can reduce the multiplication factor caused by the variability of the sun's irradiation medium. The result shows that the hyper-spectrum analysis technology is effective. Then the three methods for classifying the five types of mangrove are contrasted. The results show that the correlativity and the spectrum angle are both more accurate than the space distance. This research demonstrates that the hyper-spectrum analysis method is useful for vegetation classification. This is also shown elsewhere in research on hyper-spectrum analysis technology research [16, 17]. In this research, only a simple method of hyper-spectrum is used to analyze the spectrum characteristics of the mangrove, since there are also some disadvantages to the mathematical model. In order to obtain a higher precision for an accurate spectrum, the models should be modified.

3.2 Image classification

A major aim of this research is to obtain the Land Sat TM image classification by NN classification technology on the basis of the spectrum characteristics of the mangrove and other objects. The results are shown in Figs. 4a)–4c). Supervision is used in some of the research work, e.g., ISODATA classification technology is used to analyze the Land Sat TM image. The result shows that the precision of this supervision is lower than the precision of the supervised classification [3, 6]. Bands 3, 4, and 5 of the Land Sat TM are widely used in supervised classification technology. Bands 3 and 4 are the edges of the red range. The difference is more clearly seen than in the other images, i.e., using the two bands some ratios can be synthesized to improve the precision of the image. Therefore, taking the synthesis bands including 3, 4, 5 and 3/5, 5/4 is also widely used as the input data of the classification [12, 15].

The key technology of this research is NN classification technology. Its classification accuracy reaches 86.86%, which is higher than maximum parallel classification, which has an accuracy of 50.79% and the spectrum angle classification, which has an accuracy of 75.39%. However, it also has its disadvantages. Although the NN classification operation principle can be understood, its operation flow is unknown to most people, and therefore, the parameters are adjusted empirically instead of using contingent technology. This research is also based on experience. Consequently, this technology has some blindfold factors. However, as a new technology, it shows the application trend of manual intelligence technology in satellite image classification, and thus, it assists the remote sensing technology system.

Since the geographical information system (GIS), which is based on the yield survey and original maps, is effective in assisting the NN classification, it can improve the classification accuracy by geographical orientation. To date, the GIS technology has been widely used in the field of earth space science. In this research, the original map is transformed to a digital map, which is spliced into the satellite image to obtain the exact orientation. This can help to achieve the margin between the objects, and thus, facilitate enhanced accuracy. In addition, GIS can also help to orient the distinct objects as the image emendation reference. All in all, GIS is combined with the remote sensing and builds up the 3S technology system together with GPS.

The whole research area involves diversification, and the mangrove in Shan-Kou Guangxi, P. R. China is the densest such community in China. It distributes evenly along the shoreline, and manifests as zonal. In the whole area, the mangrove is the standard dominant community according to its predominance index, and its landscape characteristic is constant with few gaps. The shrimp pond in this area also obviously differs from other objects. The mangrove can be precisely delineated from other items, but the five varieties of mangrove are hard to delineate from each other. This is due to the fact that their reflectivity is very similar, and the difference cannot be realized by the Land Sat TM satellite image.

3.3 The Acquirement of the Landscape Index

By statistical calculation, the acreage is found to be 8673 km^2. The Landscape Diversity Index is 0.8708. This result shows that the distribution of the landscape types in the research area is relatively uniform. The predominance index of the mangrove is −1.5850, and this indicates that the area and the distribution of the mangrove are sparse in the research area, but the vegetation on the land is the predominant colony, with its predominance index being 2.2563. The uniformity index of the mangrove is 1.7789, i.e., the uniformity level is relatively high, although it is lower than the uniformity level of the land vegetation, which is 2.4562. The Landscape Fragmentation Index of the mangrove is 0.0325, and the assembly index is 0.6854. That shows that the distribution of the mangrove is even. All of these indices show that the mangrove in Shankou, Guangxi, P. R. China is relatively intact.

3.4 Precision Analysis

Some accurate area data of Ying-luo Harbor is obtained from mangrove reserve, and this area has good vegetation coverage, high congregation, low forest fragmentation. Therefore, the mangrove of Ying-luo Harbor is set as the precision analysis area. The image of the area is shown in Fig. 5a). Following this, the image is defined by the maximum parallel classification, spectrum angle classification and NN classification. The processing result are given in Figs. 5b)–

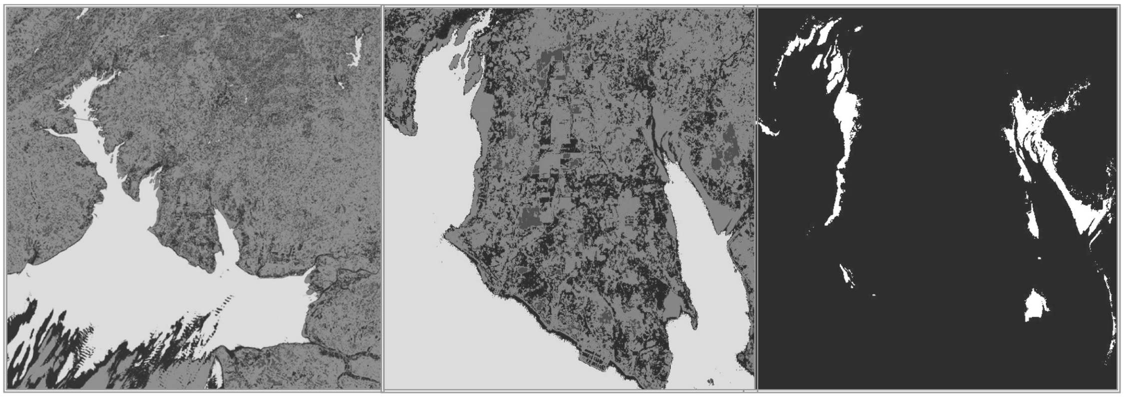

Figure 4. (a) NN classification image of the mangrove in Beihai City, (b) NN classification image of the mangrove in the Shankou mangrove reserve, and (c) The mangrove distribution in the Shankou mangrove resource protection section.

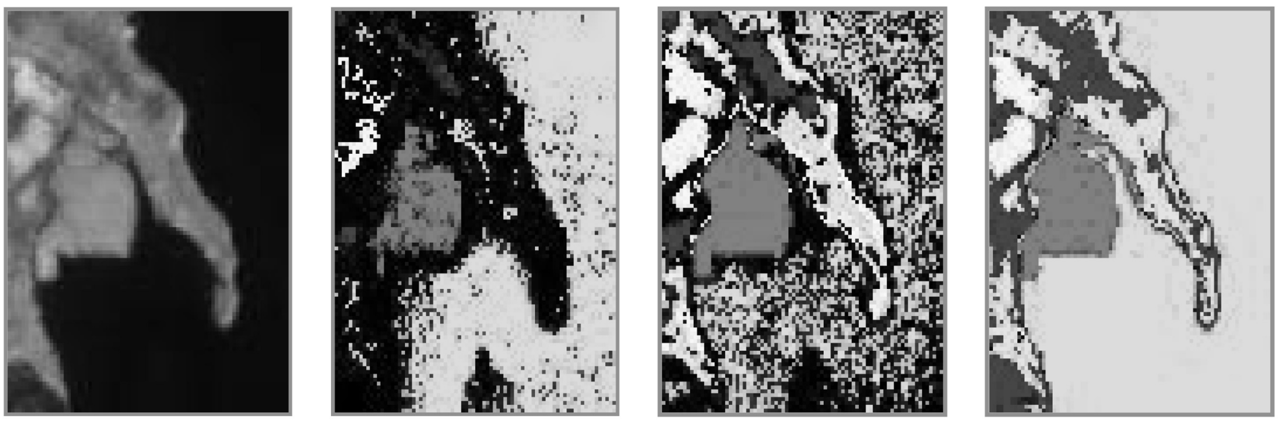

Figure 5. (a) The original satellite image of Ying-luo, (b) The result of the maximum parallel classification, (c) The result of the spectrum angle classification, and (d) The result of the NN classification.

5d). The red area represents mangrove, and the classification precision is configured by A according to Eq. (18):

$$A = N_c / N_m \tag{18}$$

where A is classification precision, N_c is the number of the mangrove units which are classified, and N_m is the actual number of mangrove units. By statistical operation, the classification precision is summarized in Tab. 1. The result of the contrast shows that the NN classification precision is optimum at 86.86% (this is larger than the precision of maximum parallel classification at 50.79%, and the precision of the spectrum angle classification, which is 75.39%).

Table 1. Precision of the classification.

Classification	Standard area	Maximum parallel	Spectrum angle	NN
The unit number	951	483	717	826
Precision, (%)	100	50.79	75.39	86.86

4 Conclusions

This research includes the original spectral data achievement methods, hyper-spectrum analysis technology, geographical information system technology and NN classification technology. These have all been used to build up the system to facilitate remote sensing acquirement technology for the landscape distribution.

Hyper-spectrum analysis technology is the base of this classification, and its advantages include the elimination of noise by logarithmic transformation and differential transform. The result shows that this method can improve the classification accuracy significantly. Another part of the study has shown that the difference between different grassland types and different plants is significant and the influence of environmental factors on plants spectra is great. Thus, it can be seen that Hyper Spectral Remote Sensing has enormous potential in its application in physiology and biochemistry of grassland plants, grassland investigation and monitoring [2, 7].

The NN classification is supported by 1:50000 topographic maps and layout maps of the mangrove resource protection section and the result of hyper-spectrum analysis technology of the spectral curves. Artificial neural network model for mangrove classification is established on the basis of selecting input-output units, pre-treating data, determining transfer functions and choosing the training functions. All the parameters are achieved by restricted functions. According the principle of NN classification, the conjunction weights of the neural network are continuously modified layer by layer from the output layer to the input layer in the process of neural network training to reduce the errors between the anticipated and actual outputs. The results show that: (1) the bigger the output layer of network, the greater the learning ability, (2) the learning ability still depends on the selection for samples, and (3) very good results can be reached while the method is being applied to classification. Maximum likelihood classifier (MLC) is the most widely used and effective classification method. The study shows that the overall accuracy of maximum likelihood is ca. 50.79%, while the overall accuracies of the spectral angle mapping and neural network are 75.39% and 86.86% respectively. A further part of the study has shown that the overall accuracy of maximum likelihood is ca. 84.89%, and the Kappa coefficient is 0.74. Finally, the overall accuracies of binary encoding, neural networking and spectral angle mapping are 87.12%, 88.75% and 90.41%, respectively [16, 17].

Acknowledgements

This work was supported by the Dalian Marine University and National Marine Environment Monitoring Center, Dalian, P. R. China, One hundred-Talent Plan of the Chinese Academy of Sciences (CAS), CAS – The Local Government Cooperative Project, and the CAS/SAFEA International Partnership Program for Creative Research Teams. The authors would like to thank Prof. Mufit Bahadir, Editor-in-Chief, Prof. Senesi Nicola, Editor and the three referees for critical comments on the submission.

References

[1] M. U. Chaudhury, Digital Analysis of Remote Sensing Data Monitoring the Ecological Status of the Mangrove Forests of Sunderbans in Bangladesh, *23rd Int. Symp. on Remote Sensing of the Environment*, Bangkok, Thailand **1990**.

[2] H.-Q. Fan, *Mangrove – The Defense of the Seashore*, Beijing Science Press, Beijing **2000**.

[3] Y.-M. Fan, Hyper Spectral Properties Analysis of Grassland Types in Xinjiang, *Acta Pratacul. Sci.* **2006**, *23*, 15 – 18.

[4] D. Gory, S. Zisman, C. Corves, Mapping of the Mangroves of Belize, Technical Report, University of Edinburgh **1990**, pp. 123 – 126.

[5] J.-L. Chen, Retrieval of Reed Canopy Using the Neural Network Method, *Remote Sens. Land Res.* **2008**, *2*, 62 – 67.

[6] H.-Y. Ding, Z.-F. Bian, Remote Sensed Image Super-resolution Reconstruction Based on a BP Neural Network, *Comput. Eng. Appl.* **2008**, *44 (1)*, 171 – 172.

[7] D.-X. Zhang, Comparison Study of Land Use/Land Cover Classification Based on the Airborne Imaging Spectrometer Data in Yixing, *Sci. Geograph. Sin.* **2004**, *24 (2)*, 193 – 198.

[8] M. Guo, Study on Landscape Fragmentation of Arid Region Oasis Based on Remote Sensing and GIS – A Case Study of the Jinta Oasis, *J. Desert Res.* **2004**, *24 (2)*, 201 – 206.

[9] J. Gao, A Comparative Study on Spatial and Spectral Resolutions of Satellite Data in Mapping Mangrove Forests, *Int. J. Remote Sens.* **2005**, *19*, 23 – 27.

[10] J.-C. Luo, C.-H. Zhou, ANN Remote Sensing Classification Model and Its Integration Approach with Geo-Knowledge, *Sci. Geograph. Sin.* **2001**, *5 (2)*, 122 – 129.

[11] W.-L. Peng, *An Introduction to Remote Sensing*, Beijing Higher Education Press, Beijing **2002**, pp. 260 – 261.

[12] J.-T. Tou, R. C. Gonzalez, *Pattern Recognition Principles*, Addison-Wesley, Reading, MA **1974**, pp. 56 – 59.

[13] J. J. Wang, Supervised Classification Neural Network Saltpan, *Ocean Technol.* **2005**, *24 (1)*, 67 – 71.

[14] A. C. Woodfine, *North East Sumatra Prawn Project*, *Remote Sensing Component*, Final Report to Natural Resources Institute/Overseas Development Agency, December **1991**, pp. 67 – 69.

[15] X.-S. Liu, Remote Sensing Classification of Forest Vegetation Based on Artificial Neural Network, *Forest Res. Manage.* **2005**, *1*, 51 – 54.

[16] F. Wu, The Research on Image Classification of Remote Sensing Based on Neural Networks, *Sci. Technol. Inf. Surv. Mapping* **2008**, *63*, 8 – 11.

[17] T.-G. Zhou, Y. Su, Fuzzy Quantification Multi-layer Feed-forward Neural Networks Remote Sensing Image Vegetation Classification, *J. Southwest China Normal Uni.* **2006**, *18*, 1037 – 1040.

